NASA Technical Memorandum 107385

An Experimental Device for Generating High Frequency Perturbations in Supersonic Wind Tunnels

Kevin J. Melcher
Lewis Research Center
Cleveland, Ohio

and

Mounir B. Ibrahim
Cleveland State University
Cleveland, Ohio

Prepared for the
International Congress on Fluid Dynamics and Propulsion
cosponsored by the American Society of Mechanical Engineers and Cairo University
Cairo, Egypt, December 29–31, 1996

National Aeronautics and
Space Administration

AN EXPERIMENTAL DEVICE FOR GENERATING HIGH FREQUENCY PERTURBATIONS IN SUPERSONIC WIND TUNNELS

Kevin J. Melcher
NASA Lewis Research Center
Cleveland, Ohio 44135

Mounir B. Ibrahim
Department of Mechanical Engineering
Cleveland State University
Cleveland, Ohio 44115

Abstract

This paper describes the analytical study of a device that has been proposed as a mechanism for generating gust-like perturbations in supersonic wind tunnels. The device is envisioned as a means to experimentally validate dynamic models and control systems designed for high-speed inlets. The proposed gust generator is composed of two flat trapezoidal plates that modify the properties of the flow ingested by the inlet. One plate may be oscillated to generate small perturbations in the flow. The other plate is held stationary to maintain a constant angle-of-attack. Using an idealized approach, design equations and performance maps for the new device were developed from the compressible flow relations. A two-dimensional CFD code was used to confirm the correctness of these results. The idealized approach was then used to design and evaluate a new gust generator for a 3.05-meter by 3.05-meter (10-foot by 10-foot) supersonic wind tunnel.

Nomenclature

Symbol	Description
A	amplitude
C_P	coefficient of pressure
D	inlet diameter
H	height of uniform flow field
H	angular momentum
$\dot{\mathsf{H}}$	torque
I	mass moment of inertia
L	length parameter
M	Mach number
W	plate width
dm	differential element of mass
f	frequency (Hertz)
t	time
x	longitudinal coordinate, measured in the direction of the flow
y	horizontal coordinate, measured perpendicular to the direction of the flow
z	vertical coordinate, measured perpendicular to the direction of the flow

Greek

Symbols	Description
Θ	angular position
$\dot{\Theta}$	angular velocity
$\ddot{\Theta}$	angular acceleration
α	angle-of-attack
β	yaw angle
δ_{i-j}	turning angle, flow deflection, or change in flow angle between regions i and j
δM	Mach number perturbation, $\delta M=M(t)-M(0)$
δP_T	total pressure perturbation, $\delta P_T=(P_T(t)-P_T(0))/P_T(0)$
θ_i	angle of the flow in region i relative to a fixed horizontal reference frame
σ_{i-j}	angle of the shock between regions i and j measured relative to the flow in region i
ω	frequency (radians/second)

Subscripts	Description
CM	center of mass
GP	gust plate parameter

Subscripts	Description
hinge	point where two plates touch
inlet	plane where flow first impinges on the inlet centerbody
max	maximum parameter value
min	minimum parameter value
nom	nominal parameter value
yy	generic axis for moment of inertia

Introduction

In recent years the international aerospace community has shown renewed interest in the development of a new generation of supersonic transport aircraft. The propulsion systems being developed for these aircraft (Figure 1) are typified by a low-bypass, subsonic turbofan connected to a mixed compression inlet. Flow enters the inlet at supersonic speeds and is reduced to subsonic velocities by a normal shock before entering the engine. In order to insure safe, efficient operation, the normal shock must remain inside the inlet despite unexpected atmospheric perturbations. Expulsion of the normal shock, a phenomena know as unstart, can have catastrophic consequences during flight. An inlet control system is required to avoid and/or minimize the impact of the unstart phenomena on aircraft operation.

In order to properly design a controller for the inlet, some knowledge of the flow dynamics is required. Preliminary knowledge is often obtained from time-accurate simulations which are then used for initial validation of the control laws. Final validation is accomplished experimentally. Proper experimental results will produce data that characterize the inlet dynamics with (i.e., closed-loop) and without (i.e., open-loop) the control. Data from open-loop tests are also useful for validating simulations which may then be used to refine control strategies. Closed-loop tests provide a mechanism for tuning and validating the control against actual hardware.

The data required for dynamic validation usually takes one of two forms, based on the form of the excitation. If the excitation is a step disturbance, the time responses of measured variables, typically static pressures, are used to evaluate the analytical models. If the excitation is a sine wave with continuously varying frequency, then the time response data is analyzed using spectral methods to obtain the system response in the frequency domain. In order to obtain useful data in either case, it is important for the highest excitation frequency to meet or exceed the corner frequency (bandwidth) of the propulsion system.

Historically, experimental data describing the inlet dynamics has been obtained by exciting the freestream flow upstream of the inlet, or by exciting the internal subsonic flow field. A number of devices have been successfully used to perturb the internal subsonic flow producing frequency response data as high as 2,200 radians per second (350 Hz) in test rigs (Bogar, 1983) and 1,260 radians per second (200 Hz) in sub-scale inlets (Wasserbauer, 1968). The devices used to perturb subsonic flow cannot be used to perturb the supersonic flow ingested by the inlet. Attempts to obtain the frequency response of high speed inlets to

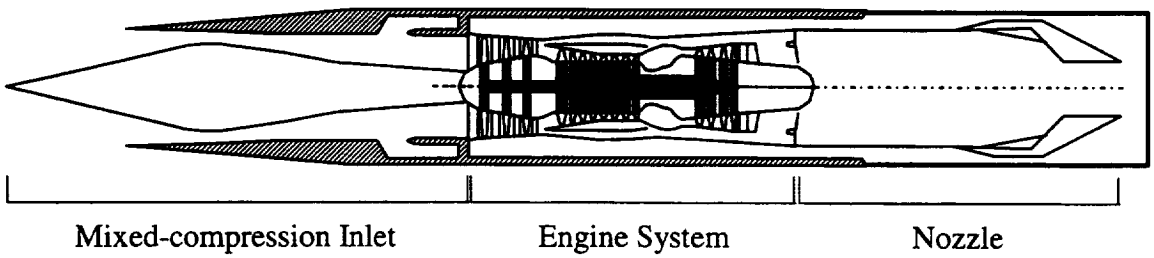

Figure 1. Typical High-Speed Inlet-Engine Configuration

high frequency changes in freestream supersonic flow have been largely unsuccessful. The problems and difficulties that arise are best illustrated by a review of the reports documenting those attempts.

In 1951, Fox (1951) produced continuously varying inlet Mach numbers in a constant Mach number tunnel by using oblique shocks originating from the leading edge of a flat, trapezoidal plate mounted below and forward of an inlet. By changing the angle of the inlet/plate assembly, he was able to change the strength of the shock wave and, consequently, the inlet Mach number. Although the results reported by Fox were strictly steady-state, they provided a foundation for future dynamics and control studies.

Hurrell (1955) evaluated the response of a ramjet with a closed-loop control to changes in the upstream Mach number using Fox's approach. He carried the approach one step further when he measured the transient response of the ramjet while changing the angle of the inlet/plate assembly relative to the flow. Unfortunately, the slow moving assembly was "not fast enough to impose noticeable errors from the set point." The change in inlet total pressure during the disturbance is not documented. From Hurrell's results, it can be shown that less than 1½ degrees of turning will produce the reported change in Mach number (from 1.84 to 1.79 in 0.6 seconds) with a negligible change in the total pressure.

Wasserbauer & Whipple (1968) also used a flat, trapezoidal plate to generate changes in the flow upstream of the inlet. However, they mounted and actuated the inlet and the "gust plate" independently. By oscillating the gust plate ±½ degree about the horizontal, they were able to generate sinusoidal freestream disturbances at 75 radians per second (12 Hz). At a tunnel Mach number of 3.0, this oscillation produced a 0.05 change in inlet Mach number, a 1 degree change in inlet angle-of-attack, and a negligible change in inlet total pressure.

Sanders (1974) tried a different method of perturbing the freestream supersonic flow. He placed a rectangular, flat plate in the tunnel throat and rotated it from a vertical to horizontal position in 15 milliseconds. This device produced a decrease in Mach number from 2.57 to 2.42, a change in local airflow angle from -3.9 degrees to -1.0 degree, and an increase in total pressure recovery from 0.955 to 0.991. The bandwidth (corner frequency) of this device was only about 8 Hz.

Cole and Hingst (1978) reported the results of an analytical study in which they investigated four devices for potential use as gust generators: a triangular air foil, tunnel throat modulation (e.g., flex wall or collapsible centerbody), a flat plate, and the blast wave from a shock tube. They concluded that, in order to simulate atmospheric-like disturbances, the gust generator should produce relatively uniform flow field perturbations with little or no change in angle of attack. Furthermore, the disturbance should be composed of a decrease in Mach number of at least 0.05 Mach and a change in total pressure of at least 8 percent. Cole and Hingst found that the devices included in this study could not meet their gust generator requirements.

Of the devices just discussed, the gust plate used by Wasserbauer and Whipple produces the most uniform flow field. Since it provides a basis for the new gust generator design, a slightly expanded review of the device is in order.

The Gust Plate

The device currently used as a gust generator at the National Aeronautics and Space Administration's Lewis Research Center is the "gust plate" first used by Wasserbauer and Whipple. Although this device does not meet the requirements defined by Cole and Hingst, it has been used to obtain a limited amount of data for validation of computer simulations and control methodologies.

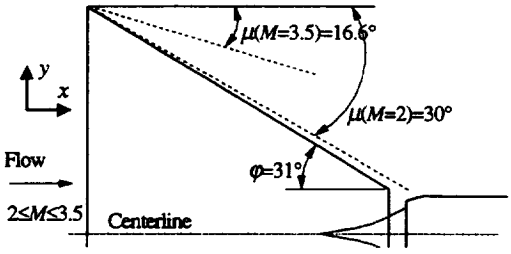

(a) Horizontal Plane

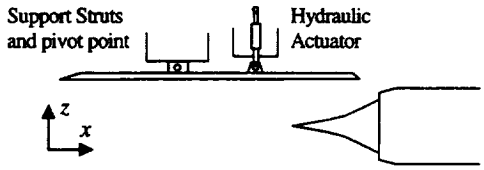

(b) Vertical Plane

Figure 2. NASA Lewis Gust Plate.

In the horizontal plane (Figure 2a), the gust plate has a trapezoidal shape that keeps Mach waves generated by the leading edge corners from interfering with the flow under the plate. The 31 degree sweep angle is 1 degree larger than the Mach angle resulting from a 2.0 freestream Mach number, the lowest Mach number at which the tunnel operates.

The pivots for the support struts (Figure 2b) have been placed at an axial coordinate approximately corresponding to the center of mass. By locating the hinges close to the center of mass, inertial effects of the mass are minimized and the frequency response maximized.

As a disturbance generator, the gust plate has three main deficiencies. First, it produces unacceptable changes in inlet angle-of-attack. Second, it does not produce total pressure perturbations with acceptable amplitude. And, third, it has insufficient frequency bandwidth due primarily to its large size and weight.

Summary of Gust Generator Requirements

The requirements used to assess the acceptability of the new gust generator are based both on the capabilities of the original gust plate and the gust criteria of Cole and Hingst. These requirements, listed in Table I and detailed by Melcher (1996), are briefly described as follows.

The requirements for maximum inlet diameter and maximum plate width ensure that the new device will meet the same geometry constraints as the original gust plate. The first requirement guarantees that the new device will support tests of small scale inlets up to 51 cm (20 inches) in diameter. The second requirement insures that the new device will fit in the wind tunnel without developing wall boundary layer interactions. The next three requirements, beginning with the Mach perturbation, are obtained directly from Cole and Hingst (1978). Realistically, the frequency bandwidth requirement is a function of inlet size; smaller inlets will have higher bandwidth requirements. So, the device will be more useful if the bandwidth greatly exceeds this requirement. The constraint on changes in angle-of-attack is designed to allow for some flexibility in the gust generator design. High-speed inlets are normally designed to accommodate a change in angle-of-attack of at least 1 degree. The final requirement is based

Table I. Summary of Requirements for Proposed Gust Generator.

Requirement	Description
$D_{inlet} \leq 50.8$	Maximum Inlet Diameter, centimeters
$W_{max} \leq 274.3$	Maximum Plate Width, centimeters
$\delta M_{inlet} \geq 0.05$	Amplitude for Mach Perturbation at 0.1 Hz
$\delta P_{T,inlet} \geq 0.08$	Amplitude for Total Pressure Perturbation at 0.1 Hz
$f_{max} \geq 70$	Frequency Bandwidth, Hertz
$-0.1 \leq \alpha \leq 0.1$	Change in Angle-of-attack, degrees
$2.1 \leq M_1 \leq 2.4$	Mach Range for the Inlet

on a desire to maximize the frequency response of the proposed device. Minimizing the Mach range of interest will increase the frequency bandwidth by decreasing the size of the plate.

Description of Proposed Gust Generator

The rest of this paper describes a new device proposed for use as a gust generator. The new device is composed of two flat trapezoidal plates. The orientation of the plates in the vertical plane is shown in (Figure 3). The new device uses two plates connected by a flexible joint or hinge to modify the flow ingested by the inlet. Plate 1 is designed to meet perturbation requirements. It will rotate about the hinge line creating perturbations in the flow. Plate 2 is designed to meet requirements for a constant angle-of-attack. There will be a region of uniform flow under each plate with direction of the flow parallel to the plate. Therefore, holding both the inlet and plate 2 stationary will result in a constant angle-of-attack regardless of perturbations in the flow caused by plate 1. Further analysis will determine if the device is able to meet the other requirements.

Compressible Flow Analysis in the Horizontal Plane

The bulk of the analysis for the proposed disturbance device has been devoted to the rather complex flow field in the vertical plane. However, an understanding of the flow in the horizontal plane is also required in order to minimize the overall size of the plate.

The plates require a trapezoidal shape in the horizontal plane based on the Mach wave considerations used to design the original gust plate (Figure 2a). The lower bound on the sweep angle for each plate may be calculated from the Mach angle as follows:

$$\varphi > \mu = \sin^{-1}\frac{1}{M}, \quad M \geq 1 \qquad (1)$$

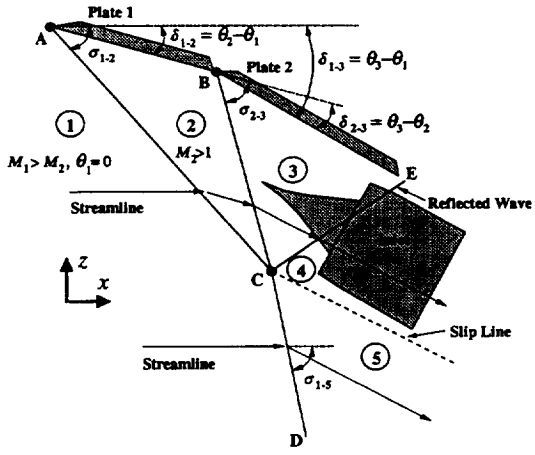

Figure 3. Flow Field Diagram for Proposed Gust Generator (Vertical Plane).

From the inverse relationship between Mach number and sweep angle, it is obvious that Low Mach numbers will tend to decrease the disturbance bandwidth by increasing the plate width, and consequently, the size and mass. This will be an important consideration in subsequent attempts to maximize the bandwidth of the proposed gust generator.

Compressible Flow Analysis in the Vertical Plane

The character of the flow field for the proposed gust generator is analogous to the general case where supersonic flow is compressed through more than one angle generating a family of oblique shocks that coalesce. A description of the flow field for such a system is given by Anderson (1982). In Figure 3, that approach is applied to the proposed disturbance generator.

A weak oblique shock, **AC**, is formed when the supersonic flow in region 1 encounters plate 1 with initial deflection, $\delta_{1\text{-}2}$, and is turned. The deflection sets the flow angle in region 2 parallel to the plate. A second oblique, **BC**, is formed when the flow in region 2 encounters plate 2 with deflection, $\delta_{2\text{-}3}$. This deflection sets the flow angle in region 3 which is also parallel to the plate. Because the second shock has a lower

upstream Mach number than the first shock, it has a steeper angle and eventually the two shocks coalesce into **CD**. Now, the properties in region 3 have gone through two shocks, but the properties in region 5 have gone through only one shock. Therefore, the entropy in regions 3 and 5 must be different and a slip line, originating at the point of intersection, will exist downstream of the shock structure. Furthermore, for the slip line to exist, the static pressure and the flow angle in regions 4 and 5 must be equal. However, it is generally impossible to find a single shock that will result in the same pressure and flow angle as the two intermediate shocks. Anderson notes that nature resolves this problem by inserting, a reflected wave, **CE**, that originates from the intersection of oblique shocks **AC** and **BC**. This wave will take a form that appropriately resolves the flow. For the work reported here, the wave is an expansion that effects the flow field in regions 4 and 5 by turning it slightly away from the plate. Should the wave intersect plate 2, a reflected wave will form at that point of intersection to turn the flow back parallel to the plate.

It is of interest here to consider the placement of an inlet in the flow field. The inlet should not be placed in region 2 because it is the same as operating the inlet with a single plate. A single plate can not meet the established requirements. It would also be unacceptable for the inlet to span regions 4 and 5. Here, the flow properties are uniform only when the two plate angles are the same (i.e., $\theta_2=\theta_3$). If a slip line exists, the static pressure and flow angle in the two regions will be equivalent, however, the Mach number and temperature will not. Finally, the inlet should not be placed solely in region 5 as perturbations in the angle of plate 1 produce negligible changes in the flow properties. This leaves regions 3 and 4 as the logical place to locate an inlet.

It is evident from Figure 3 that the structure of the flow field is not only a function of the

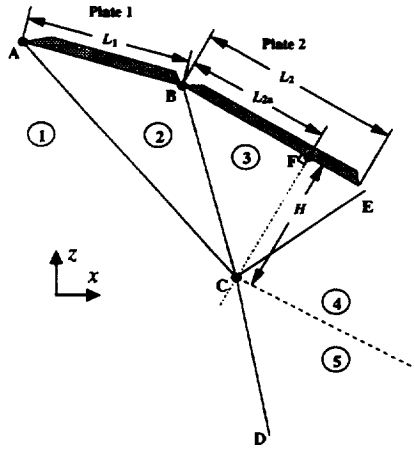

Figure 4. Length Parameters for Proposed Gust Generator (Vertical Plane).

freestream Mach number and the plate angles, but the plate lengths as well. In Figure 4, L_1 and L_2 represent the respective lengths of plates 1 and 2. H is a distance measured perpendicular to plate 2 from the bottom of the plate to the intersection of the two shocks. L_{2a} is the distance from point **B**, the leading edge of plate 2, to point **F**, the point at which the perpendicular through **C** intersects the bottom of the plate. This distance, L_{2a}, is the minimum length that results in a uniform flow field of height, H.

Consider an inlet placed in region 3 or 4 with axis parallel to plate 2. The inlet diameter will be bounded by the distance between Plate 2 and the slip-line when measured perpendicular to the plate, **CF**. The location of point **C**, and hence the slip-line, is dependent on four parameters: the freestream Mach number, M_1, the two turning angles, $\delta_{1\text{-}2}$ and $\delta_{2\text{-}3}$, and the length of Plate 1, L_1. The Mach number and the turning angles will determine the angle of the oblique shocks and hence the angles of triangle **ABC**. It is then a matter of simple geometry to show that H and L_1 are directly proportional. This means that the gust generator size, mass, and frequency bandwidth are all proportional to the largest inlet diameter of interest.

Results from Solution of the Compressible Flow Equations

A set of equations describing the idealized flow field of the proposed gust generator is given by Melcher (1996). In this section, maps resulting from the solution of these steady-state isentropic flow and oblique shock equations are discussed. The maps (Figures 5 through 9) show how properties of the flow vary as a function of freestream Mach number and plate angle.

The flow property maps were developed by first selecting a nominal inlet Mach number and a nominal angle for plate 1. $M_{3,nom}$=2.35 was selected as a typical inlet Mach number for supersonic transports. A horizontal orientation, $\theta_{2,nom}=\delta_{1\text{-}2,nom}=0$, was chosen for the plate 1 because it simplifies the maps.

After choosing values for $M_{3,nom}$ and $\delta_{1\text{-}2,nom}$, several nominal values for the angle of plate 2 were chosen such that $\theta_{3,nom}=\delta_{1\text{-}3,nom}$=10, 12, 14, 16, and 18 degrees. Given the nominal angle of plate 1, each value of $\delta_{1\text{-}3}$ requires a unique freestream Mach number to match the nominal inlet Mach number of 2.35 (i.e., $M_{1,nom}$=2.812, 2.929, 3.060, 3.209, and 3.384). With the freestream Mach number and the angle of plate 2 held constant, the flow field properties may be calculated as the plate 1 is varied from 0 degrees to θ_3.

The Mach perturbation for region 3 is shown as a function of $\delta_{1\text{-}2}$ and $\delta_{1\text{-}3}$ in Figure 5. Two observations can be made from this result. First, it appears that values of $\delta_{1\text{-}3}$ larger than 15 degrees will be needed to meet amplitude requirements of 0.05 Mach. It is worth noting here, that blockage and geometry considerations may make it impossible to operate the wind tunnel with the hardware at positioned at these relatively large angles. Also, while higher values of $\delta_{1\text{-}3}$ allow for larger perturbations in the flow, they require a higher freestream Mach number. In general, the wind tunnel should be operated at the lowest possible Mach number in order to minimize power requirements and reduce

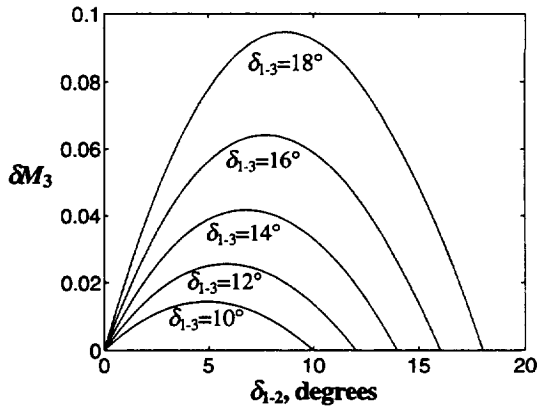

Figure 5. Variations in Region 3 Mach Perturbation as a Function of the Initial and Total Flow Deflection.

cost. With this in mind, the gust generator design should be optimized to operate with plate 2 at the most acute angle which allows amplitude requirements to be met.

The second observation stems from the fact that minimizing the amplitude of an actuator system will tend to increase its bandwidth. The map suggests that plate 1 should be perturbed about a nominal operating point near the extrema of $\delta_{1\text{-}2}$. Operating plate 1 near $\delta_{1\text{-}2}$=0 (horizontal) or $\delta_{1\text{-}2}=\delta_{1\text{-}3}$ will provide the best possibility of meeting amplitude and bandwidth requirements due to the larger gradients.

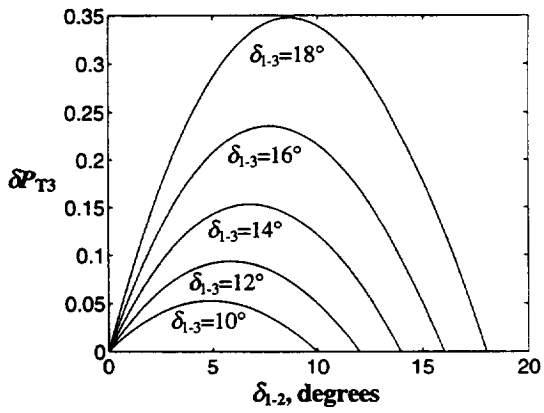

Figure 6. Variations in Region 3 Total Pressure Perturbation as a Function of the Initial and Total Flow Deflection.

Figure 6 shows the variation in total pressure perturbation. Again, there are two observations. First, the required amplitude may be obtained at values of $\delta_{1\text{-}3}$ as low as 12 degrees. This is much lower than the value required for Mach perturbations. Therefore, in designing the device for a given operating range, it appears sufficient to focus on the amplitude of the Mach perturbation. The second observation is essentially the same observation made in the previous paragraph. Namely, plate 1 should be operated near the extrema of $\delta_{1\text{-}2}$ where the gradients are larger.

The change in the direction of flow from region 3 to region 4, $\delta_{3\text{-}4}$, is shown in Figure 7. Note that changes in the direction of flow during a perturbation are minimized by operating plate 1 near either end of its range. Also note that the nonuniformity between regions 3 and 4 may be reduced by operating the device at more acute total turning angles.

Figures 8 and 9 show how the length ratios L_1/H and L_{2a}/H vary as a function of deflection angles $\delta_{1\text{-}2}$ and $\delta_{1\text{-}3}$. As with previous results, these plots support operating plate 1 at the lowest possible value of M_1 and $\delta_{1\text{-}3}$. However, unlike the previous plots, these results suggest that plate 1 should be perturbed about an

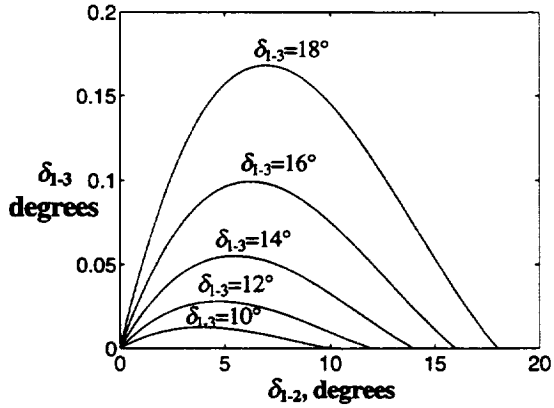

Figure 7. Variations in the Change in Flow Angle Between Regions 3 and 4 as a Function of the Initial and Total Flow Deflection.

operating point strictly near $\delta_{1\text{-}2} = \delta_{1\text{-}3}$. It is near this point that the plate lengths (and thus moments of inertia) are minimized. Therefore, when $\delta_{1\text{-}2,nom} \cong \delta_{1\text{-}3}$, the bandwidth ought to be the greatest.

CFD Validation of Compressible Flow Analysis

Validation is an important part of the modeling process. This is especially true when models become complex and improper assumptions or solution procedures may result in the wrong conclusions. As a means of validating the

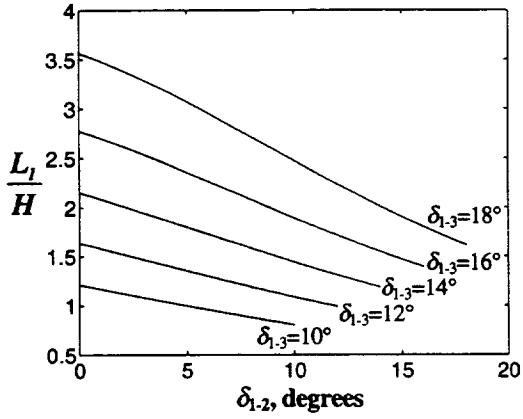

Figure 8. Variations in the Length of Plate 1 as a Function of the Initial and Total Flow Deflection.

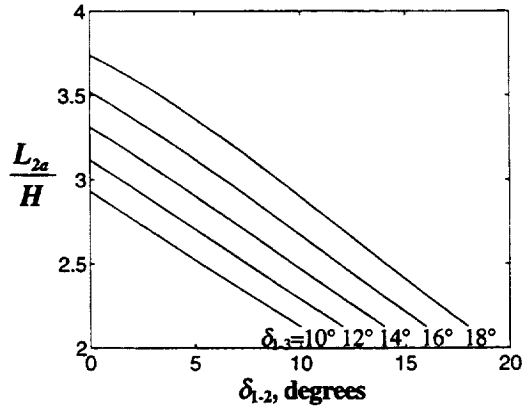

Figure 9. Variations in the Length of Plate 2 as a Function of the Initial and Total Flow Deflection.

idealized results, a CFD study was performed. The objective of the study was to obtain reasonably accurate results from a two-dimensional (2D) CFD code that would independently verify the correctness of the idealized compressible flow calculations. A detailed discussion of the CFD study is given by Melcher (1996). In this section, the results of that study are summarized.

The geometry of the gust generator was defined by placing two plates in a rectangular flow field representative of a wind tunnel. In order to keep the gust generator grid relatively simple, the two plates were oriented in the flow field so that the trailing edge of plate 1 was always touching the leading edge of plate 2. The flow field was then divided into four blocks as shown in Figure 10. Six grids (A through F) of varying resolution (coarse through fine) were used before an acceptable solution was achieved. Both quantitative and qualitative comparisons were made between the compressible flow solutions and the 2D CFD results.

Table II. Summary of Pressure Coefficient Calculations for $\delta_{1\text{-}2}$=12° and $\delta_{1\text{-}3}$=16°.

		LOWER SURFACE	
		Plate 1	Plate 2
GRID	C_P(CF)	0.2020	0.305
C	C_P(2D)	0.1811	0.303
	Δ	-0.0208	-0.00235
	%Δ	-10.3	-0.8
E	C_P(2D)	0.1986	0.305
	Δ	-0.0033	-0.0007
	%Δ	-1.7	-0.2
F	C_P(2D)	0.2002	0.305
	Δ	-0.0017	-0.0005
	%Δ	-0.9	-0.2

Symbol	Description
(CF)	Compressible Flow Result
(2D)	2D CFD Result
Δ	C_P(2D)-C_P(CF)
%Δ	100*Δ/C_P(CF)

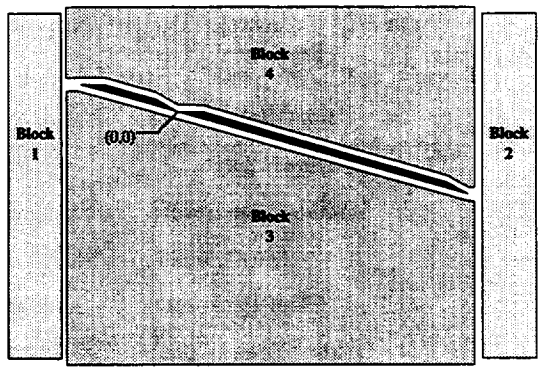

Figure 10. Exploded View of Block Structure for CFD Analysis.

Quantitative comparisons were made using the pressure coefficient, C_P, for the bottom of each plate. Table II shows the result of these calculations for several grids when $\delta_{1\text{-}2}$=12 degrees and $\delta_{1\text{-}3}$=16 degrees. There is good agreement as results from the compressible flow solution and the F-grid (highest resolution) vary by less than 1 percent.

Qualitative comparisons were made by plotting the compressible flow solution on top of the 2D CFD results. Due to space constraints, the various plots are not reproduced here. However, shock angles and flow properties predicted by the compressible flow solution were in good agreement with results from both grids E and F.

Bandwidth Estimation

The results presented in figures 5 through 9 show that the new gust generator can be designed to meet six of the seven gust generator requirements listed in Table I. The only requirement not quantitatively addressed, the bandwidth requirement, will be discussed in this section.

An actuator system is needed to assess whether or not the new gust generator can meet bandwidth requirements. Prior to that, a detailed structural analysis ought to be performed. The structural analysis should minimize weight while maintaining high strength and stiffness.

Table III. Geometric Design Parameters for Plate 1.

Parameter	Value
Leading Edge Bevel	15 degrees
Trailing Edge Bevel	15 degrees
Plate Length	91.68 cm
Plate Thickness	3.89 cm
Leading Edge Width	266.47 cm
Trailing Edge Width	197.61 cm
Lower Surface Area	2.128 m^2
Plate Volume	0.070 m^3
Center of Mass	44.18 cm

Table IV. Geometric Design Parameters for Plate 2.

Parameter	Value
Leading Edge Bevel	15 degrees
Trailing Edge Bevel	15 degrees
Plate Length	127.92 cm
Plate Thickness	3.89 cm
Leading Edge Width	197.61 cm
Trailing Edge Width	50.80 cm
Lower Surface Area	1.589 m^2
Plate Volume	0.055 m^3
Center of Mass	53.89 cm

Since these detailed analysis are outside the scope of this study, a number of assumptions were made. In lieu of an actuator system design, the actuator system for the gust plate is used to estimate the bandwidth of the new gust generator. The new device was designed using the same thickness and bevel angles as the original gust plate. However, four different materials were considered as structural materials for the new gust generator.

A new gust generator design that meets the previously specified requirements is detailed by Melcher (1996). Geometric parameters resulting from the design process are given in Tables III and IV. In order to complete the design, an amplitude was needed for the change in angle of plate 1. During the design process, an amplitude of ±2 degrees was needed to provide required changes in Mach number and total pressure. That same value is used in this section to compute bandwidth estimates.

In order to provide an estimate of the frequency bandwidth, it was necessary to compute the mass moment of inertia for both the gust plate and plate 1 of the proposed device. The mass moment of inertia is a measure of resistance to rotational acceleration. The mass moment of inertia for the gust plate is 1.86×10^7 Newton-centimeters squared (4,503 pound-feet squared). Table V shows values for the mass moment of inertia of plate 1 when composed of stainless steel (SS), titanium (Ti), aluminum (Al), and a typical graphite composite (Gr). The mass moments of inertia were computed using equations that describe the surface of the plate, including the effect of the leading and trailing edge bevels. The moments of inertia shown for each of the four materials are for two axes of rotation. The first axis of rotation is the hinge line where the two connected plates touch (Figure 3). Consideration is also given to a second axis parallel to the hinge line. This axis is located 7 cm (2.75 inches) above the center

Table V. Plate 1 Parameter Values for Four Different Structural Materials.

	SS	Ti	Al	Gr
Density				
kg/m^3	7,889	4,567	2,768	1,384
(lb/in^3)	(0.285)	(0.165)	(0.100)	(0.050)
Weight				
N	550	318	193	96
(lb)	(1,211)	(701)	(425)	(213)
I_{hinge}				
$N \cdot m^2$	1,499	868	526	263
($lb \cdot ft^2$)	(3,628)	(2,100)	(1,273)	(636)
I_{CM}				
$N \cdot m^2$	283	164	99	50
($lb \cdot ft^2$)	(684)	(396)	(240)	(120)

of mass (i.e., same location as the gust plate). It was considered because rotation about the center of mass yields the minimum mass moment of inertia and should yield the highest frequency bandwidth. It is also likely that the center of pressure will be near this point which will minimize any aerodynamic moments. Note that in order for plate 1 to rotate about the second axis, the two plates must be physically disconnected. A CFD study should be performed on this configuration to evaluate the interaction of the plates with the flow.

Estimates of the frequency bandwidth were obtained by considering the angular sinusoidal perturbation of plate 1 about the previously defined axes. Equation (2) describes the angular position of the plate as a function of time. Equations (3) and (4) describe the angular velocity and the angular acceleration, respectively.

$$\Theta(t) = A\sin(\omega t) \tag{2}$$

$$\dot{\Theta}(t) = A\omega\cos(\omega t) \tag{3}$$

$$\ddot{\Theta}(t) = -A\omega^2\sin(\omega t +) \tag{4}$$

A maximum value for these parameters may be calculated as shown in equations (5), (6) and (7) using values for the gust plate.

$$\Theta_{max} = A = \tfrac{1}{2}^\circ = 8.7267\times10^{-3}\ \text{rad} \tag{5}$$

$$\dot{\Theta}_{max} = A\omega_{max} = 0.65797\ \text{rad/sec} \tag{6}$$

$$\ddot{\Theta}_{max} = A\omega_{max}^2 = 49.610\ \text{rad/sec}^2 \tag{7}$$

Here, 75 radians/second (12 Hz) is used as the value for maximum excitation frequency. This is the highest frequency reported by Wasserbauer and Whipple (1968).

For the flat plate in question, equations (8) and (9) show the relationship of the angular velocity, angular acceleration, and moment of inertia to angular momentum and torque.

$$H = I_{yy}\dot{\Theta}_y \tag{8}$$

$$\dot{H} = I_{yy}\ddot{\Theta}_y \tag{9}$$

Combining the equations with values from equations (5) through (7) and Table V, maximum values for the angular momentum and torque may be computed.

$$H_{max} = I_{GP}\dot{\Theta}_{max} = 1{,}2224\ \frac{\text{N}\cdot\text{m}^2}{\text{sec}} \tag{10}$$

$$\dot{H}_{max} = I_{GP}\ddot{\Theta}_{max} = 92{,}310\ \frac{\text{N}\cdot\text{m}^2}{\text{sec}^2} \tag{11}$$

Assuming that the actuator system can provide the level of angular momentum and angular acceleration specified in equations (10) and (11), it is then possible to determine the maximum frequency that may be attained with the proposed gust generator design. Equations (12) through (14) show the formulas needed to calculate the results displayed in Table VI.

$$A = 2^\circ = 3.4907\times10^{-2}\ \text{radians} \tag{12}$$

$$\omega_{max}(H_{max}) = \frac{H_{max}}{A\cdot I_{yy}} = \frac{35{,}073}{I_{yy}} \tag{13}$$

$$\omega_{max}(\dot{H}_{max}) = \sqrt{\frac{\dot{H}_{max}}{A\cdot I_{yy}}} = \frac{1{,}626}{I_{yy}} \tag{14}$$

The data in Table VI show that, due to torque limitations, the gust plate actuator system cannot drive the new gust generator at frequencies meeting bandwidth requirements. Only one case meets the 70 Hz bandwidth requirement. That case requires that the gust generator be made of graphite composite, that plate 1 be rotated about an axis near the center-of-mass, and that the bandwidth be limited by angular momentum instead of torque. Part of the reason that there is not a more significant increase in bandwidth is that increases due a smaller moment of inertia are offset by requirements for a larger amplitude.

Table VI. Estimates of Frequency Bandwidth for Various Structural Materials and Axis of Rotation

	SS	Ti	Al	Gr
Axis 1 (hinge line)				
$\omega_{max}=F(H_{max})$ radians/sec (Hz)	23 (4)	40 (6)	67 (11)	133 (21)
$\omega_{max}=F(\dot{H}_{max})$ radians/sec (Hz)	42 (7)	55 (9)	71 (11)	100 (16)
Axis 2 (center of mass)				
$\omega_{max}=F(H_{max})$ radians/sec (Hz)	124 (20)	214 (34)	353 (56)	707 (112)
$\omega_{max}=F(\dot{H}_{max})$ radians/sec (Hz)	97 (15)	127 (20)	163 (26)	230 (37)

Rather than suggesting that the proposed gust generator will not work, the data in Table VI highlight the need for a high speed actuator designed specifically for this application. However, if an actuator system design that provides suitable frequency response for a single oscillating plate proves to be unfeasible, it is possible to further reduce the inertia of plate 1 by dividing it width-wise into several independently actuated sections. The resulting increase in bandwidth will not come without a price. In order to maintain a uniform flow field, the actuator control must move all plate sections in phase throughout the required frequency domain.

Concluding Remarks

This work was motivated by need for an experimental device to test control systems for high speed inlets. Over the past 40 years, a number of devices have been investigated for their ability to generate high frequency gust-like perturbations in supersonic flow. To date, no device has been found which meets the gust generator requirements defined by Cole and Hingst. The purpose of this research was to propose and investigate the feasibility of a new gust generator. The study focused primarily on aspects of the problem related to the fluid mechanics, although, some mechanical design considerations were also taken into account.

The results in this paper show that the proposed device can meet the gust generator requirements based on geometry and flow field considerations. They also show that the more detailed structural and actuator system designs needed to determine the ability of the device to meet bandwidth requirements are warranted.

References

Anderson, John D., Jr., 1982, "Modern Compressible Flow with Historical Perspective," McGraw-Hill Book Company, New York, NY.

Bogar, T.J., Sajben, M., and Kroutil, J.C., 1983, "Response of Supersonic Inlet to Downstream Perturbations," AIAA-83-2017.

Cole, Gary L., and Hingst, Warren R., 1978, "Investigation of Means for Perturbing the Flow Field in a Supersonic Wind Tunnel," NASA TM-78954.

Fox, J.L., 1951, "Supersonic Tunnel Investigation by Means of Inclined-Plate Technique to Determine Performance of Several Nose Inlets Over mach Range of 1.72 to 2.18," NACA RM-E50K14.

Hurrell, H.G., Vasu, G., and Dunbar, W.R., 1955, "Experimental Study of Shock Positioning Method of Ram-jet-engine Control," NACA RM E55F21.

Melcher, Kevin J., 1996, "A Method for Perturbing the Flow Field in Supersonic Wind Tunnels for Dynamic Analysis of High Speed Inlets," Masters Thesis, Cleveland State University, Cleveland, Ohio.

Sanders, B.W., Bishop, A.R., and Webb, J.A., Jr., 1974, "Gust Generator for a Supersonic Wind Tunnel," NASA TM X-3120.

Wasserbauer, Joseph F., and Whipple, Daniel L., 1968, "Experimental Investigation of the Dynamic Response of a Supersonic Inlet to External and Internal Disturbances," NASA TM X-1648.

REPORT DOCUMENTATION PAGE

Form Approved
OMB No. 0704-0188

1. AGENCY USE ONLY (Leave blank)	2. REPORT DATE	3. REPORT TYPE AND DATES COVERED
	December 1996	Technical Memorandum

4. TITLE AND SUBTITLE

An Experimental Device for Generating High Frequency Perturbations in Supersonic Wind Tunnels

5. FUNDING NUMBERS

WU-537-05-21

6. AUTHOR(S)

Kevin J. Melcher and Mounir B. Ibrahim

7. PERFORMING ORGANIZATION NAME(S) AND ADDRESS(ES)

National Aeronautics and Space Administration
Lewis Research Center
Cleveland, Ohio 44135-3191

8. PERFORMING ORGANIZATION REPORT NUMBER

E-10578

9. SPONSORING/MONITORING AGENCY NAME(S) AND ADDRESS(ES)

National Aeronautics and Space Administration
Washington, DC 20546-0001

10. SPONSORING/MONITORING AGENCY REPORT NUMBER

NASA TM-107385

11. SUPPLEMENTARY NOTES

Prepared for the International Congress on Fluid Dynamics and Propulsion cosponsored by the American Society of Mechanical Engineers and Cairo University, Cairo, Egypt, December 29-31, 1996. Kevin J. Melcher, NASA Lewis Research Center, and Mounir B. Ibrahim, Cleveland State University, Department of Mechanical Engineering, Cleveland, Ohio 44115. Responsible person, Kevin J. Melcher, organization code 5530, (216) 433-3743.

12a. DISTRIBUTION/AVAILABILITY STATEMENT

Unclassified - Unlimited
Subject Categories 01 and 09

This publication is available from the NASA Center for AeroSpace Information, (301) 621-0390.

12b. DISTRIBUTION CODE

13. ABSTRACT *(Maximum 200 words)*

This paper describes the analytical study of a device that has been proposed as a mechanism for generating gust-like perturbations in supersonic wind tunnels. The device is envisioned as a means to experimentally validate dynamic models and control systems designed for high-speed inlets. The proposed gust generator is composed of two flat trapezoidal plates that modify the properties of the flow ingested by the inlet. One plate may be oscillated to generate small perturbations in the flow. The other plate is held stationary to maintain a constant angle-of-attack. Using an idealized approach, design equations and performance maps for the new device were developed from the compressible flow relations. A two-dimensional CFD code was used to confirm the correctness of these results. The idealized approach was then used to design and evaluate a new gust generator for a 3.05-meter by 3.05-meter (10-foot by 10-foot) supersonic wind tunnel.

14. SUBJECT TERMS	15. NUMBER OF PAGES
Disturbance generator; Gust generator; Supersonic wind tunnel; Control validation	14
	16. PRICE CODE: A03

17. SECURITY CLASSIFICATION OF REPORT	18. SECURITY CLASSIFICATION OF THIS PAGE	19. SECURITY CLASSIFICATION OF ABSTRACT	20. LIMITATION OF ABSTRACT
Unclassified	Unclassified	Unclassified	